

Magnetoplasmons in layered graphene structures

Oleg L. Berman,¹ Godfrey Gumbs², and Yurii E. Lozovik,³

¹*Physics Department, New York City College of Technology of the City University of New York,
300 Jay Street, Brooklyn, NY 11201*

²*Department of Physics and Astronomy, Hunter College of the City University of New York,
695 Park Avenue, New York, NY 10021*

³*Institute of Spectroscopy, Russian Academy of Sciences, 142190 Troitsk, Moscow Region, Russia
(Dated: November 6, 2018)*

We calculate the dispersion equations for magnetoplasmons in a single layer, a pair of parallel layers, a graphite bilayer and a superlattice of graphene layers in a perpendicular magnetic field. We demonstrate the feasibility of a drift-induced instability of magnetoplasmons. The magnetoplasmon instability in a superlattice is enhanced compared to a single graphene layer. The energies of the unstable magnetoplasmons could be in the terahertz (THz) part of the electromagnetic spectrum. The enhanced instability makes superlattice graphene a potential source of THz radiation.

PACS numbers: 71.35.Ji, 71.35.Lk, 71.35.-y

I. INTRODUCTION

Recent advances in fabrication techniques have made it possible to produce graphene, which is a two-dimensional (2D) honeycomb lattice of carbon atoms forming the basic planar structure in graphite [1]. Graphene has stimulated considerable theoretical interest as a semi-metal whose electron effective mass may be described by an unusual massless Dirac-fermion band structure. Several novel many-body effects in graphene have been investigated [2, 3]. The theory of Weiss oscillations in the magnetoplasmon spectrum of Dirac electrons in graphene has been developed in Ref. [4]. The magnetoplasmon excitations in graphene for filling factors $\nu < 6$ has been calculated in Ref. [5]. In recent experiments, the integer quantum Hall effect (IQHE) has been reported [6]. Quantum Hall ferromagnetism in graphene has been investigated from a theoretical point of view [7]. Graphene has a number of interesting properties as a result of its unusual band structure which is linear near two inequivalent points (K and K') in the Brillouin zone. In the presence of a magnetic field, the graphene structure shifts both the Shubnikov-de Haas oscillations [8] as well as the step pattern of the IQHE [9]. Both these effects have recently been reported experimentally [6]. The spectrum of plasmon excitations in a single graphene layer embedded in a material with effective dielectric constant ϵ_b in the absence of an external magnetic field, has been calculated in [10]. In this paper, we show that features, such as charge density oscillations, arise when a magnetic field is applied.

This paper is organized as follows. In Sec. II, we analyze the magnetoplasmon spectrum for a single graphene layer. The collective charge density excitations in a strong magnetic field for a graphite bilayer and a bilayer graphene are calculated in Secs. III and IV, respectively. The enhancement of the magnetoplasmon instability in an infinite periodic graphene superlattice is investigated in Sec. V. In these calculations, we assume that there is no tunneling between the graphene layers forming the su-

perlattice. The results of our numerical calculations are presented in for each structure investigated. A brief discussion of plasmon instabilities in graphene is presented in Sec. VI.

II. A SINGLE GRAPHENE LAYER

Let us first consider electrons in a single graphene layer in the xy -plane in a perpendicular magnetic field \mathbf{B} parallel to the positive z axis. Here, we neglect the Zeeman splitting and assume valley energy degeneracy, describing the eigenstates by two pseudo spins [9, 11]. We have an effective 2×2 matrix Hamiltonian $\hat{H}_{(0)}$ whose diagonal elements are zero and whose off-diagonal elements are $\hat{\pi}_x \pm i\hat{\pi}_y$ where $\hat{\pi} = -i\hbar\nabla + e\mathbf{A}$, $-e$ is the electron charge, \mathbf{A} is the vector potential, $v_F = \sqrt{3}at/(2\hbar)$ is the Fermi velocity with $a = 2.566\text{\AA}$ denoting the lattice constant, and $t \approx 2.71\text{ eV}$ is the overlap integral between nearest-neighbor carbon atoms [9].

Choosing $\mathbf{A} = (0, Bx, 0)$, the eigenfunctions of $\hat{H}_{(0)}$ are labeled by $\alpha = \{k_y, n, s(n)\}$, where $n = 0, 1, 2, \dots$ is the Landau level index, k_y is the electron wave vector in the y -direction, and $s(n)$, which is defined by $s(n) = 0$ for $n = 0$ and $s(n) = \pm 1$ for $n > 0$, labels the conduction (+1) and valence (-1 and 0) band, respectively. The eigenfunction $\psi_\alpha(\mathbf{r})$ is given by a spinor $\psi_\alpha(x, y)$ with components given by [9] $\psi_\alpha^{(1)} = C_n e^{ik_y y} s(n) i^{n-1} \Phi_{n-1}(x + l_H^2 k_y) / \sqrt{L_y}$ and $\psi_\alpha^{(2)} = C_n e^{ik_y y} i^n \Phi_n(x + l_H^2 k_y) / \sqrt{L_y}$. Here, $l_H = \sqrt{\hbar/eB}$, and L_y is a normalization length. We have $C_n = 1$ for $n = 0$, $C_n = 1/\sqrt{2}$ for $n > 0$ and $\Phi_n(x) = (2^n n! \sqrt{\pi} l_H)^{-1/2} e^{-(x/l_H)^2/2} H_n(x/l_H)$, where $H_n(x)$ is a Hermite polynomial. The eigenenergies are given by $\epsilon_\alpha = s(n)\epsilon_n = s(n)(\hbar v_F/l_H)\sqrt{2n}$, for which successive levels are not equally separated.

The dynamic dielectric function in RPA [13] is given by $\epsilon(q, \omega) = 1 - V_c(q)\Pi(q, \omega)$, where q is the in-plane wave vector, $V_c(q) = 2\pi e^2/(\epsilon_s q)$ is the 2D Coulomb interaction

and the 2D polarization function is

$$\begin{aligned} \Pi(q, \omega) &= \frac{g_s g_v}{2\pi l_H^2} \sum_{n=0}^{\infty} \sum_{n'=0}^{\infty} \sum_{s(n), s'(n')} \frac{f_{s(n)n} - f_{s'(n')n'}}{\hbar\omega + \epsilon_{s(n)n} - \epsilon_{s'(n')n'}} \\ &\times F_{ss'}(n, n', q), \end{aligned} \quad (1)$$

where $f_{s(n)n}$ is the Fermi-Dirac function, $F_{ss'}(n, n')$ arises from the overlap of eigenstates and is given by

$$\begin{aligned} F_{ss'}(n, n', q) &= C_{n_1}^2 C_{n_2}^2 \left[-\frac{q^2 l_H^2}{2} \right]^{n_1 - n_2} \frac{1}{|(n_1 - n_2)!|^2} \\ &\times \left(s_1(n_1) s_2(n_2) \left| \frac{(n_1 - 1)!}{(n_2 - 1)!} \right| + \left| \frac{n_1!}{n_2!} \right| \right). \end{aligned} \quad (2)$$

The magnetoplasmon dispersion relation for a single graphene layer was obtained by seeking the solutions of $\epsilon(q, \omega) = 0$. The highest valence band is full and all others empty at $T = 0$ K. Transitions to the lowest five Landau levels in the conduction and valence bands were the only single-particle excitations included in our calculations. Fig. 1 (a) is the solution of the dispersion equation for a single layer of graphene when the imaginary part of the plasmon frequency is zero. In this case, the plasmons are self-sustaining oscillations except when they enter the particle-hole mode region where they undergo a loss due to Landau damping. In Fig. 1 (b), we plot the solutions of the dispersion when the frequency is complex for which the real part that is linear in q and exists only where the magnetoplasmon in Fig. 1 (a) has negative group velocity. The real and imaginary parts of the frequency are denoted by ω_R and $\omega_I > 0$, respectively. The loss corresponds to finite imaginary part of frequency. This instability after excitation is due to a transfer of energy back from a magnetoplasmon to an electric current which excites it, thereby making this collective mode unstable (see Fig 1 (b)). Thus, we have a non-zero imaginary part of the frequency for a single graphene layer in a magnetic field. The non-zero imaginary part for collective excitations for a 2D electron gas (2DEG) in semiconductors has been established, out only for several layers of semiconductor [17, 18, 19, 20]. See also [17, 18, 19, 20].

The negative group velocity for $ql_H > 1$ is caused by the magnetic field [21]. We used the same parameters are employed in calculating Fig. 1, but we summed over a larger number of Landau levels in the conduction and valence bands. Qualitatively, the results are the same. The main differences are that the number of single-particle excitation lines which are allowed is increased and the frequency of the highest mode which is, of course, affected by the number of Landau levels included in the sum. However, the lower branches of collective modes do not change significantly. Therefore, including in the calculations the five lowest Landau levels in the conduction and valence bands is justified.

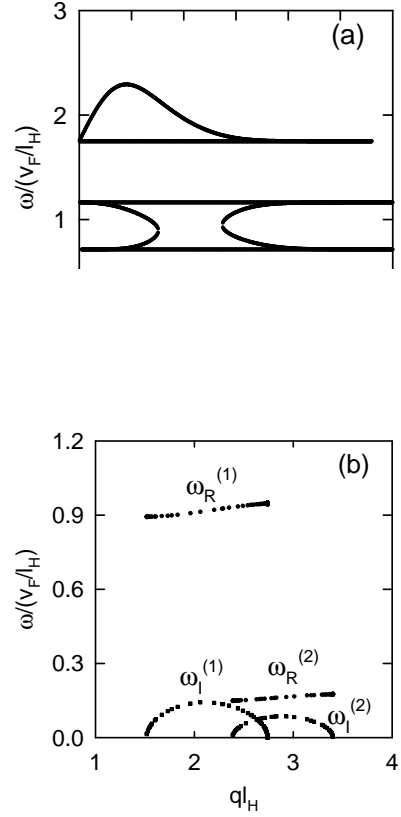


FIG. 1: Magnetoplasmon excitation energy as a function of wave vector, in units of l_H^{-1} , in a single graphene layer. (a) Real frequency solution. (b) The real and imaginary parts of the frequency satisfying the dispersion equation.

III. A GRAPHITE BILAYER

While the electron effective mass in a graphene single layer is zero, a graphite bilayer consisting of a pair of parallel graphite layers with inter-planar separation $c/2$ implies finite electron mass. The electron spectrum a graphite bilayer in a magnetic field is very much different from the case of a single graphene layer. This is caused by interlayer hopping. Here, $c/a = 2.802$ with $a = 2.566 \text{ \AA}$ denoting the lattice constant [22]. The nearest-neighbor tight-binding approximation yields a gapless state with parabolic bands touching at the K and K' points instead of conical bands [23, 24]. A graphite bilayer can be treated as a gapless semiconductor. The eigenfunction $\psi_\alpha(\mathbf{r})$ of an electron in a graphite bilayer in a perpendicular magnetic field is given for low-lying energy excitations by [24]

$$\psi_\alpha^{(b)}(x, y) = \frac{C_n^{(b)}}{\sqrt{L_y}} e^{ik_y y} \begin{pmatrix} \Phi_n(x + l_H^2 k_y) \\ s(n) Q_n \Phi_{n-2}(x + l_H^2 k_y) \end{pmatrix}, \quad (3)$$

where $\alpha = \{k_y, n, s(n)\}$, $C_n^{(b)} = 1$ when $n = 0$ or $n = 1$ and $C_n^{(b)} = 1/\sqrt{2}$ when $n \geq 2$. Also, $Q_n = 0$ when $n = 0$ or $n = 1$ and $Q_n = 1$ when $n \geq 2$ and $\Phi_n(x)$ is

defined above. The corresponding eigenenergy is $\epsilon_\alpha^{(b)} = s(n)\epsilon_n^{(b)} = s(n)\hbar\omega_c\sqrt{n(n-1)}$, where $\omega_c = eB/m$ with $m = \gamma_1/(2v^2)$, $\gamma_1 = 0.39$ eV and $v = 8 \times 10^5$ m/s [24] (compare to the electron spectrum in magnetic field in a single graphene layer presented above).

Following the procedure described above, it can be seen that for the RPA dielectric function $\epsilon^{(b)}(q, \omega)$ for a graphite bilayer, we must replace the polarization by $\Pi^{(b)}(q, \omega)$ instead of $\Pi(q, \omega)$. This is obtained from Eq. (1) by means of the eigenspectrum $\epsilon_{n,s(n)}^{(b)}$ instead of $\epsilon_{n,s(n)}$. In this case, the form factor $F_{ss'}(n, n', q)$ is replaced by

$$\begin{aligned} F_{ss'}^{(b)}(n, n', q) = & A \left(C_n^{(b)} C_{n'}^{(b)} \right)^2 \left(\left| \int_{-\infty}^{\infty} dx \exp[iq_x x] \right. \right. \\ & \times \left. \Phi_n(x) \Phi_{n'}(x + l_H^2 q_y) \right|^2 \\ & + \left| s(n) s'(n') Q_n Q_{n'} \int_{-\infty}^{\infty} dx \exp[iq_x x] \Phi_{n-2}(x) \right. \\ & \times \left. \Phi_{n'-2}(x + l_H^2 q_y) \right|^2 \Big). \end{aligned} \quad (4)$$

The eigenfunction of bilayer Bernal graphene presented in Eq. (3) was obtained in Ref. [24] by taking into account the interlayer Coulomb interactions whose dominant contributions are included. These are due to nearest-neighbor intralayer hopping (see Fig. 1 in Ref. 24). The interlayer Coulomb interactions are included in Eq. (4) since they are contained in the wavefunctions of Eq. (3), entering into the overlap integral Eq. (4). In Fig. 2, we present the dispersion relation. The four straight lines correspond to the single-electron transitions between different Landau levels. Three curved lines are the undamped magnetoplasmon excitations. For a range of wave vectors the group velocity is negative due to the magnetic field, a result similar to those in a single graphene layer. The transfer of energy between collective excitations and electrons appears only when the charged particle velocity has the same value as the phase velocity of the collective mode.

IV. A BILAYER GRAPHENE

For bilayer graphene with layer separation, D and no interlayer hopping, we have the dispersion equation [10, 15, 30, 31]

$$\begin{aligned} & \sinh^2(qD) \left(2V_c(q) \Pi_{11}(q, \omega) - \frac{\varepsilon_1}{\varepsilon_b} - \coth(qD) \right) \\ & \times \left(2V_c(q) \Pi_{22}(q, \omega) - \frac{\varepsilon_2}{\varepsilon_b} - \coth(qD) \right) = 1, \end{aligned} \quad (5)$$

where $\Pi_{jj}(q, \omega)$ is the polarization function of the charge carriers on the first $j = 1$ or the second $j = 2$ graphene layer defined by Eq. (1). We observe that in the limit

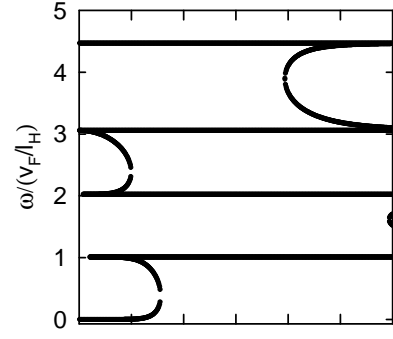


FIG. 2: Dispersion relation for bilayer graphene at $T = 0$ K with separation $D = l_H$. Only the highest Landau level in the valence is occupied and completely full.

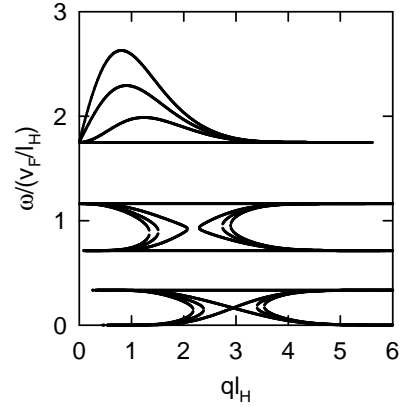


FIG. 3: Magnetoplasmon dispersion relation for bilayer graphene at $T = 0$ K with separation $D = l_H$. Only the highest Landau level in the valence is occupied and completely full.

$qD \gg 1$, Eq. (5) reduces to the dispersion equation for magnetoplasmons in a single graphene layer. If $\Pi_{11}(q, \omega) = \Pi_{22}(q, \omega) = \Pi(q, \omega)$, and $\varepsilon_1 = \varepsilon_2 = \varepsilon_b$, then we get from Eq. (5):

$$\begin{aligned} & [(2V_c(q)\Pi(q, \omega) - 1)(1 - e^{-2qD}) - (1 + e^{-2qD})] \\ & = \pm 2e^{-qD}. \end{aligned} \quad (6)$$

The dispersion relation for magnetoplasmons in bilayer graphene is presented in Fig. 3. These results show that each originally degenerate magnetoplasmon mode in each layer of an isolated single graphene layer is shifted from their value by the interlayer Coulomb interaction. For a range of wave vectors the group velocity is negative due to the magnetic field, analogous to the magnetoplasmon modes in a single graphene layer. A region of instability also exists for bilayer graphene.

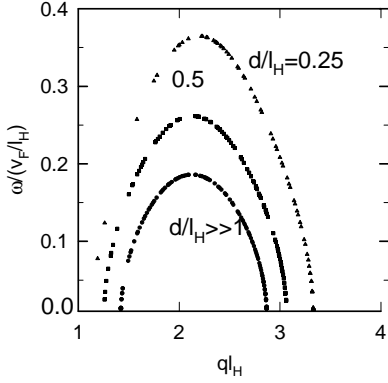


FIG. 4: The imaginary part of the magnetoplasmon energy in a single graphene layer compared to the results for an infinite superlattice of graphene layers at $\nu = 1$, $k_z l_H = 0.1$, for superlattice period $d = 0.25l_H$, $d = 0.5l_H$, and $d \gg l_H$.

V. AN INFINITE PERIODIC GRAPHENE SUPERLATTICE

Let us consider an infinite periodic graphene superlattice consisting of 2D layers parallel to the xy -plane and located at $z = ld$ where $l = 0, \pm 1, \pm 2, \dots, \pm \infty$ and d is the period. The layers are embedded in a medium with background dielectric constant ϵ_b . The dispersion equation may be calculated in RPA in the same way described in Refs. [14, 32]. It may be shown that the dispersion relation for magnetoplasmons in a superlattice is obtained by solving $1 - V_c(q)\Pi(q, \omega)S(q, k_z) = 0$, where $\Pi(q, \omega)$ is the polarization function for a single graphene layer defined by Eqs. (1)-(2). Also, $S(q, k_z)$ is the structure factor determining the phase coherence of the collective excitations in different layers given by $S(q, k_z) = \sinh(qd)/(\cosh(qd) - \cos(k_z d))$. Note that the periodicity ensures that $S(q, k_z)$ is independent of the layer index l . Also, the effective-mass model is employed to represent the low-frequency electron band structure of the layered graphene. At small separations, the low-energy bands may be modified by the interlayer atomic interactions. In this case, the Landau levels may be dispersive in the k_z wave vector.

We have solved the magnetoplasmon dispersion equation in the complex frequency plane. We present only the imaginary part of the solution for various values of d/l_H in Fig. 4 for $k_z l_H = 0.1$.

The results of our numerical calculations for an infinite graphene superlattice show that there are magnetoplasmon modes and modes independent of the wave vector corresponding to single-particle transitions between Landau levels. Due to a magnetic field, the group velocity is negative, as seen over a given range of wave vectors. This is analogous to the magnetoplasmons in a single graphene layer. Energy transfer from a charged particle to the collective modes occurs only when the charged particle's velocity has the same value as the phase velocity of the collective mode. The most energetic collective

mode increases for small wave vectors $ql_H < 1$ and is Landau damped for large wave vectors. It is shown in Fig. 4, that the imaginary part of the collective mode frequencies responsible for the magnetoplasmon instability is appreciably enhanced in an infinite superlattice of graphene layers compared to the single layer. Both the real and imaginary parts of magnetoplasmon frequencies are much larger in a graphene superlattice than in a single graphene layer due to the superposition of the collective modes corresponding to oscillations from different layers occurring in-phase. The amplification of the collective mode frequencies increases when a/l_H decreases. According to Fig. 4, it is clearly shown that the amplification of magnetoplasmons is increased as a/l_H is reduced. When $a/l_H = 0.25$ the magnetoplasmon frequencies are about twice as large compare to these at $a/l_H \rightarrow \infty$. For $a/l_H = 0.5$, these corresponding frequencies are larger by a factor of 1.5 relative to the result when $a/l_H \rightarrow \infty$.

While the 2D energy band is not suitable for describing the low-frequency electronic properties of bulk graphite [33], the calculated magnetoplasmon frequencies obtained from our superlattice model are valid. This is the case because the separation between neighboring graphene layers in the superlattice is much larger than in bulk graphite. In a graphene superlattice, the distance between graphene layers can be sufficiently large, e.g., as assumed in Fig. 4 $d = 0.25l_H$, $d = 0.5l_H$, or $d = l_H$ (e.g., $l_H = 66\text{\AA}$ at $B = 15\text{T}$), which is large compared to the distance between carbon layers in bulk graphite which is $c/2$, where $c/a = 2.802$ with $a = 2.566\text{\AA}$ denoting the lattice constant. The significance of this enhanced magnetoplasmon instability in superlattices of graphene for device applications may lie in possibly utilizing the energy of the amplified plasma modes for electromagnetic radiation in the THz regime, leading to a potential new source of radiation based on superlattices of graphene layers. For example, with an applied magnetic field $B = 10\text{T}$, corresponding to filling factor $\nu = 1$, the magnetoplasmon frequency is about 3.6THz . Moreover, the advantage of such sources of THz radiation is the fact that the frequencies corresponding to magnetoplasmon instability leading to THz electromagnetic radiation decrease when applied magnetic field increases and the parameter a/l_H decreases which results in the possibilities of controlling the THz radiation frequencies by changing the applied magnetic field.

VI. DISCUSSION

We emphasize the appearance of a magnetoplasmon instability in a single graphene layer even without the application of an in-plane current driving the charge carriers. This instability corresponds to the finite imaginary part in the frequency of the collective excitations in Fig. 1. There is a plasmon instability in a bilayer semiconductor without an in-plane current appears only in a very small region (compared to the Fermi wave vector) of

the wave vector [34]. This difference in the spectrum of collective excitations in graphene structures compared to layered semiconductors is caused by the screening properties of the dielectric function in graphene [10, 35] and

2D semiconductors [21].

Acknowledgments: This work is supported by contract # FA9453-07-C-0207 of AFRL.

-
- [1] K. S. Novoselov *et al.*, Science **306**, 666 (2004); Y. Zhang *et al.*, Phys. Rev. Lett. **94**, 176803 (2005).
 - [2] Kenneth W. -K. Shung, Phys. Rev. B **34**, 979 (1986).
 - [3] S. Das Sarma, E. H. Hwang, and W.-K. Tse, Phys. Rev. B **75**, 121406(R) (2007).
 - [4] M. Tahir and K. Sabeeh, Phys. Rev. B **76**, 195416 (2007).
 - [5] Yu. A. Bychkov, and G. Martinez, Phys. Rev. B **77**, 125417 (2008).
 - [6] K. S. Novoselov *et al.*, Nature (London) **438**, 197 (2005); Y. B. Zhang *et al.*, Nature (London) **438**, 201 (2005); Y. Zhang *et al.*, Phys. Rev. Lett. **96**, 136806 (2006).
 - [7] K. Nomura and A. H. MacDonald, Phys. Rev. Lett. **96**, 256602 (2006).
 - [8] G. P. Mikitik and Yu. V. Sharlai, Phys. Rev. Lett. **82**, 2147 (1999).
 - [9] Y. Zheng and T. Ando, Phys. Rev. B **65**, 245420 (2002).
 - [10] E. H. Hwang and S. Das Sarma, Phys. Rev. B **75**, 205418 (2007).
 - [11] C. Tóke, P. E. Lammert, V. H. Crespi, and J. K. Jain, Phys. Rev. B **74**, 235417 (2006).
 - [12] A. Iyengar, J. Wang, H. A. Fertig, and L. Brey, Phys. Rev. B **75**, 125430 (2007).
 - [13] D. Pines, *Elementary Excitations in Solids* (Benjamin, New York, 1963).
 - [14] S. Das Sarma and J. J. Quinn, Phys. Rev. B **25**, 7603 (1982).
 - [15] A. Eguluz, T. K. Lee, J. J. Quinn, and K. W. Chiu, Phys. Rev. B **11**, 4989 (1975).
 - [16] B. N. J. Persson, Solid State Commun. **52**, 811 (1984).
 - [17] P. Bakshi, J. Cen, and K. Kempa, J. Appl. Phys. **64**, 2243 (1988).
 - [18] J. Cen, K. Kempa, and P. Bakshi, Phys. Rev. B **38**, 10051 (1988).
 - [19] K. Kempa, P. Bakshi, J. Cen, and H. Xie, Phys. Rev. B **43**, 9273 (1991).
 - [20] K. Kempa, J. Cen, and P. Bakshi, Phys. Rev. B **39**, 2852 (1989).
 - [21] K. W. Chiu and J. J. Quinn, Phys. Rev. B **9**, 4724 (1974).
 - [22] S. B. Trickey, F. Müller-Plathe, G. H. F. Diercksen, and J. C. Boettger, Phys. Rev. B **45**, 4460 (1992).
 - [23] K. S. Novoselov *et al.*, Nature Physics (London) **2**, 177 (2006).
 - [24] E. McCann and V. I. Falko, Phys. Rev. Lett. **96**, 086805 (2006).
 - [25] O. L. Berman, Yu. E. Lozovik and G. Gumbs, Phys. Rev. B **77**, 155433 (2008).
 - [26] D. W. Snoke, Science **298**, 1368 (2002).
 - [27] L. V. Butov, J. Phys.: Condens. Matter **16**, R1577 (2004).
 - [28] V. B. Timofeev and A. V. Gorbunov, J. Appl. Phys. **101**, 081708 (2007).
 - [29] J. P. Eisenstein and A. H. MacDonald, Nature **432**, 691 (2004).
 - [30] S. Das Sarma and A. Madhukar, Phys. Rev. B **23**, 805 (1981).
 - [31] G. R. Aizin and Godfrey Gumbs, Phys. Rev. B **54**, 2049 (1996).
 - [32] S. Das Sarma, Phys. Rev. B **28**, 2240 (1983).
 - [33] J.-C. Charlier, X. Gonze, and J.-P. Michenaud, Phys. Rev. B **43**, 4579 (1991).
 - [34] A. Balassis and G. Gumbs, unpublished.
 - [35] T. Ando, J. Phys. Soc. Jpn. **75**, 074716 (2006).